Metabolism and lipid mediators as regulators of innate immune cell function: implications for inflammation and immune responses

Almeida, L.

IV

IgA2 ACPA Drives a Hyper-Inflammatory Phenotype in Macrophages via ATP Synthase and COX2

Luís Almeida*[1], Alice Bacon*[2], Mohan Ghorasaini[3], Alwin J. van der Ham[1], René E. M. Toes[2], Martin Giera[3], Bart Everts#[1]

First published: 01 April 2025, European Journal of Immunology

1 – Centre for Infectious Diseases, Leiden University Medical Centre, Leiden, The Netherlands
2 – Department of Rheumatology, Leiden University Medical Centre, Leiden, The Netherlands
3 – Centre for Proteomics and Metabolomics, Leiden University Medical Centre, The Netherlands
* – These authors contributed equally
# – Corresponding author – b.everts@lumc.nl

European Journal of Immunology
DOI: 10.1002/eji.202451586

Abstract

IgA can form immune complexes (ICs) and activate myeloid cells via Fc alpha receptor-mediated signalling to secrete pro-inflammatory cytokines. It was previously described that of the two IgA subclasses (IgA1 and IgA2), IgA2 is more inflammatory than IgA1. However, the mechanisms underlying this differential proinflammatory potential remain poorly defined. Using anti-citrullinated protein IgA1 and IgA2 antibodies (ACPA) that are commonly found in rheumatoid arthritis (RA) patients and linked to chronic inflammation, we show here that, in macrophages, IgA2-ICs boost TLR-induced TNF and IL6 secretion, COX2 expression, and production of COX2-dependent lipid mediators to a higher level than IgA1-ICs. Metabolically, we found the amplification of TLR-induced cytokine production and COX2 induction by IgA2-ICs to be dependent on mitochondrial ATP synthesis, but not glycolysis. Finally, we found the potentiation of TLR-induced cytokine production by IgA-ICs to be COX2-dependent. Together this work points towards a key role for mitochondrial ATP synthesis in driving COX2 expression and subsequent IgA2-IC-dependent potentiation of TLR-induced cytokine production by macrophages. As such, our work provides new insights into the mechanisms underlying IgA2-induced inflammation in the context of RA. Thus, this may hold novel clues to be explored as therapeutic possibilities to target antibody-driven inflammation in chronic inflammatory diseases.

Introduction

IgA is the most abundant antibody in the human body (1), primarily located in mucosal tissue as a dimer, where it plays an important role in both protection and maintenance of homeostasis (2). However, IgA is also the second most common circulating antibody, where, unlike in the mucosa, it exists as both a monomer or dimer, lacking the secretory component (3). This inherent characteristic of circulatory IgA allows it to bind to Fcα-receptor I (FcαRI) expressed by myeloid cells, such as macrophages, which has been linked to induce pro-inflammatory cytokines, such as TNF and IL-6 (4).

Two subclasses of IgA exist: IgA1 and IgA2. Recent studies have described that IgA2 potentiates TLR-induced inflammatory responses in macrophages, dendritic cells (DCs), monocytes, and neutrophils more strongly than IgA1 (5–9). However, the mechanisms by which IgA2 achieves this remain to be determined. IgA1 and IgA2 differ in their glycosylation profile and hinge regions. IgA1 has two conserved N-glycosylation sites and a hinge with an O-linked glycosylation rich structure, while IgA2 has four conserved N-glycosylation sites and no O-linked sites (10,11). Although it has been suggested that differences in glycosylation affect IgA-receptor interactions (11,12), it is still unknown how this translates into altered cellular responses in myeloid cells, leading to different inflammatory outputs.

It has been established that changes in the metabolism of myeloid cells are intimately linked to their function and activation states (13,14). In the context of FcR-driven inflammatory responses, it was shown that IgA immune complexes (ICs) enhance the synthesis of proinflammatory cytokines in dendritic cells (DCs), and that this is achieved through glycolytic reprogramming (6,15). In a similar fashion, it was demonstrated that IgG boosts TLR-induced cytokine synthesis in macrophages by inducing a switch towards glycolytic metabolism (16).
Moreover, IgG-ICs have been shown to induce prostaglandin E_2 (PGE_2) synthesis in macrophages (16). It is well known that lipid mediators, such as PGE_2, play an important role in regulating inflammatory responses, including that of macrophages, through autocrine and paracrine signalling (16–20). However, it is still unknown whether differential metabolic reprogramming or COX2/PGE_2 expression play a role in the ability of IgA1 and IgA2 to induce distinct inflammatory responses.

Therefore, in this study, we aimed to investigate the difference in inflammatory potential and underlying mechanisms of IgA1 and IgA2 in human monocyte-derived macrophages in the context of TLR co-stimulation. We found that IgA2-ICs synergize more strongly with TLR stimulation than IgA1-ICs, as evidenced by higher levels of

TNF and IL-6 induction. Additionally, we show a metabolic link between IgA2 signalling and COX2 induction, whereby ATP synthase is crucial for the aforementioned effects of IgA2, but not IgA1, on macrophage activation. We also show that this IgA2-induced phenotype is associated with increased PGE_2 synthesis and, correspondingly, with an augmented expression of COX2. Finally, we describe that, by targeting COX2 activity with indomethacin, we are able to abrogate the boosting effects of IgA2 in macrophage inflammatory potential, albeit this effect seems to be independent of PGE_2.

In summary, our work links IgA2-induced inflammation, with COX-dependent mediators, and ATP Synthase activity in macrophages.

Results

IgA2 Synergizes With TLR2/1 Signalling to Induce a More Inflammatory Phenotype in Macrophages via Syk

We first aimed to assess the inflammatory potential of IgA1 and IgA2 on human macrophages. We decided to focus on IgA ACPAs, which are known to play an important role in the inflammatory response in RA. This disease is characterized by chronic inflammation of the joints, specifically the synovium. One of the hallmarks of this inflammatory environment in the synovium is the crosstalk between macrophages and ACPAs. Importantly, the levels of IgA ACPAs and rheumatoid factor specific IgA in the synovium are significantly increased in patients with RA and are associated with RA flares (21,22). Moreover, higher IgA2:IgA1 ratios have been associated with a worse disease score in RA patients (5), making IgA1 and IgA2 ACPAs highly clinically relevant to study this interaction. To do so, we employed an *in vitro* model whereby we cultured human monocyte-derived macrophages in plates pre-coated with citrullinated antigen (CCP2), and with equal concentrations of either monoclonal IgA1 or IgA2 ACPA (Fig. S1 A-C) – both having the same patient derived variable domain sequence – to simulate ACPA-ICs, in the presence or absence of PAM3CSK4 (PAM), a TLR2/1 ligand, since many danger associated molecular patterns associated with RA have been shown to signal via this TLR (23). Furthermore, we opted by differentiating macrophages with GM-CSF due to its role in RA in driving macrophage differentiation, M1-polarization, Fcα receptor expression, and subsequent inflammation and cartilage degradation (24–30). Additionally, GM-CSF has been implicated in regulating macrophage proliferation, glycolysis, lipid metabolism, and mitochondrial function (31,32). Therefore, macrophages from a GM-CSF background present themselves as a relevant model to study macrophages in the context of RA and IgA binding, along with their metabolism and inflammatory responses.

Upon dual stimulation with PAM and IgA, we found that IgA2, but not IgA1, synergized

with the TLR signalling to induce TNF and IL-6 (Fig1. A, B). In addition, COX-dependent lipid species, including PGE_2, were also more strongly upregulated following IgA2 stimulation (Fig1. C and Fig. S2 A, B). However, this was not the case for LOX-dependent species (Fig1. D). The increased production in PGE_2 was paralleled by potentiated COX2 expression (Fig1. E). Finally, we found the effect of IgA2 to be dependent on syk, a crucial mediator of FcR-signalling, as syk inhibition abrogated IgA2-driven potentiation of TLR-induced cytokine synthesis and COX2 expression, with no decrease in cell viability (Fig. S3 A-D).

Together, these data show that IgA2 has a stronger proinflammatory effect than IgA1 on macrophages and further suggest that this is syk-dependent.

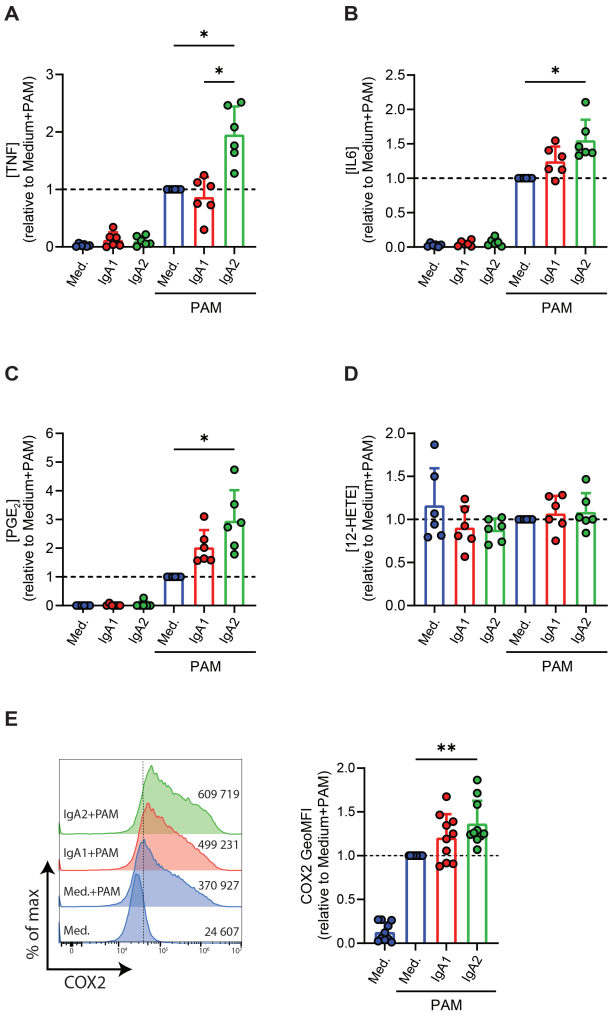

(legend on next page)

Fig1: **IgA synergizes with PAM to potentiate TLR-induced cytokine production and COX2 expression in macrophages.** Levels of (A) TNF, (B) IL-6, (C) PGE_2, and (D) 12-HETE measured in supernatants following stimulation of cells with indicated compounds. Levels of (A) TNF and (B) IL-6 were measured with ELISA as described in materials and methods. (E) Representative histogram of COX2 expression for each indicated stimulus (left); values represent the pooled average raw GeoMFI of all experiments. (Right) normalized COX2 GeoMFI of cells treated with indicated stimuli. (A)-(D) are representative plots of 6 donors from 2 independent experiments (mean ± SD). (E) is a representative plot of 10 donors from 5 independent experiments (mean ± SD). All data were analysed using a paired one-way ANOVA. * $p < 0.05$, ** $p < 0.01$.

IgA2 and PAM Co-Stimulation Induces Metabolic Changes in the Mitochondrial Compartment

Since IgA has been previously shown to reprogram DCs into a pro-inflammatory phenotype by potentiating glycolysis (15), and since PGE_2 was shown to have an effect on mitochondrial metabolism in macrophages (33), we aimed to explore whether IgA2-driven inflammatory responses were accompanied by, and dependent on, metabolic rewiring. Using a metabolic flux analyser to measure OCR (oxygen consumption rate) (Fig2. A) and ECAR (extracellular acidification rate) (Fig. S4 A), we found that IgA1 and IgA2 did not promote significant changes in glycolysis (Fig. S4 B-D), basal respiration (Fig2. B), or ATP synthesis (Fig2. C) 24h after stimulation, although IgA2-stimulated cells appeared to have a lower respiratory spare capacity (Fig2. D). This was also associated with trends towards lower expression of mitochondrial enzymes 24h following stimulation with IgA2 (Fig2. E-H), albeit no change was observed in mitochondrial membrane potential (Fig. S4 E). SCENITH assay to assess the dependence on mitochondrial metabolism and glycolytic metabolism for ATP-dependent translation, revealed no clear differences (Fig2. I-L). Together this indicates that, in human macrophages, IgA1 and IgA2, except for altered mitochondrial respiratory spare capacity, induce minor changes in core metabolic pathways.

Inhibition of Mitochondrial Respiration Abrogates the Pro-Inflammatory Effects of IgA2

Next, we evaluated whether the potentiated inflammatory profile induced by IgA2 was dependent on any core metabolic pathway activity, using various inhibitors. While blocking glycolysis with 2-Deoxy-D-Glucose (2-DG), slightly affected TNF production, blocking glycolysis with 2-DG, or fatty acid oxidation with etomoxir, did not affect the production of IL-6, nor COX2 expression (Fig. S5 A-C). Interestingly, blocking ATP Synthase with oligomycin abrogated the potentiating effects of IgA2 on both TNF (Fig3. A) and IL-6 (Fig3. B) production. Additionally, oligomycin also prevented the boosting effect of IgA2 on COX2 expression (Fig3. C). Correspondingly, oligomycin, and the general COX inhibitor indomethacin (Indo), but not 2-DG or etomoxir, were able to block IgA2-induced PGE_2 synthesis, and other COX2-dependent mediators (Fig4. A-C). Of note, there were no effects on cellular viability by the inhibitors used,

apart from minimal effects by 2-DG (Fig. S6). Interestingly, oligomycin showed no effect on IgA1-induced potentiation of COX2-derived products by TLR-stimulated macrophages (Fig4. D-F). Additionally, LOX-dependent mediators were unaffected by oligomycin treatment upon IgA2 or IgA1 stimulation (Fig4. G, H). This together suggests that the effects of IgA2 on TLR-induced cytokine production and COX2 activity are dependent on ATP Synthase activity.

The Pro-Inflammatory Effects of IgA2 Are Supported by COX2 Activity

As PGE_2 is a well-known signalling lipid in macrophages (16–20), we wondered if this IgA2-potentiated inflammatory profile was dependent on COX2 induction and subsequent PGE_2 synthesis. To test this, we stimulated cells with IgA in the presence of PAM and indomethacin. Upon inhibiting COX activity, the enhancement of IgA2 on TNF (Fig5. A) and particularly IL-6 (Fig5. B) production was reduced. Furthermore, in a similar fashion as observed with oligomycin (Fig3. B), Indomethacin not only prevented IgA2 potentiation on IL-6 production, but it also decreased the production of IL-6 by PAM in the absence of IgA, thus showing that PAM as well as the potentiated response by IgA2 requires COX2 activity for IL-6 production by these cells.

Since IgA2 was boosting COX2 expression and PGE_2 synthesis, and indomethacin reduced the pro-inflammatory effects of IgA co-stimulation with TLR2/1 and PGE_2 synthesis, we tested whether we could rescue these effects by adding PGE_2 to the medium of these cells. Interestingly, the addition of PGE_2 had no effect on the synthesis of IL-6 upon inhibition of COX with indomethacin or oligomycin (Fig. S7), indicating the synergistic effect of IgA2 and TLR2/1 on the pro-inflammatory phenotype of macrophages is dependent on COX, but possibly independent of PGE_2 synthesis.

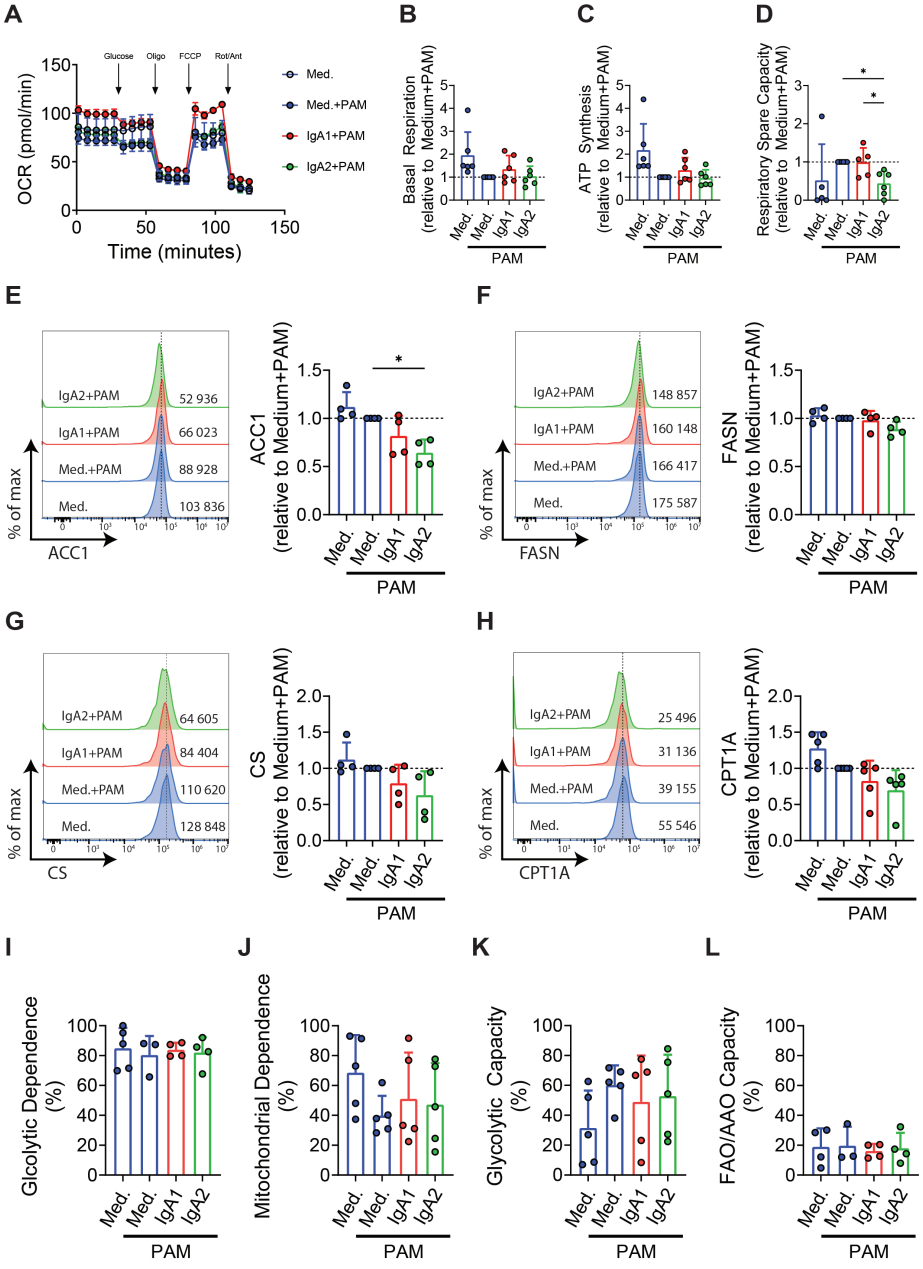

Fig2: **IgA2-PAM co-stimulation induces metabolic changes in the mitochondrial compartment.** Representative histograms (left) and normalized GeoMFI (right) of (E) ACC1, (F) FASN, (G) CS, and (H) CPT1A measured via FACS following 24h stimulation of cells with indicated stimuli. Values in histograms represent the pooled average raw GeoMFI of all experiments. (I) Glycolytic Dependence, (J) Mitochondrial Dependence, (K) Glycolytic Capacity, and (L) Fatty Acid and Amino Acid Oxidation (FAO/AAO) capacity measured using SCENITH and calculated as described in materials and methods. (A)-

(D) are representative plots of 6 donors from 3 independent experiments with outliers removed (mean ± SD). (E)-(G) are representative plots of 4 donors from 2 independent experiments (mean ± SD). (H) is a representative plot of 5 donors from 3 independent experiments (mean ± SD). (I)-(L) are representative plots of 5 donors from 2 independent experiments (mean ± SD). All data were analysed using a paired one-way ANOVA. * $p < 0.05$.

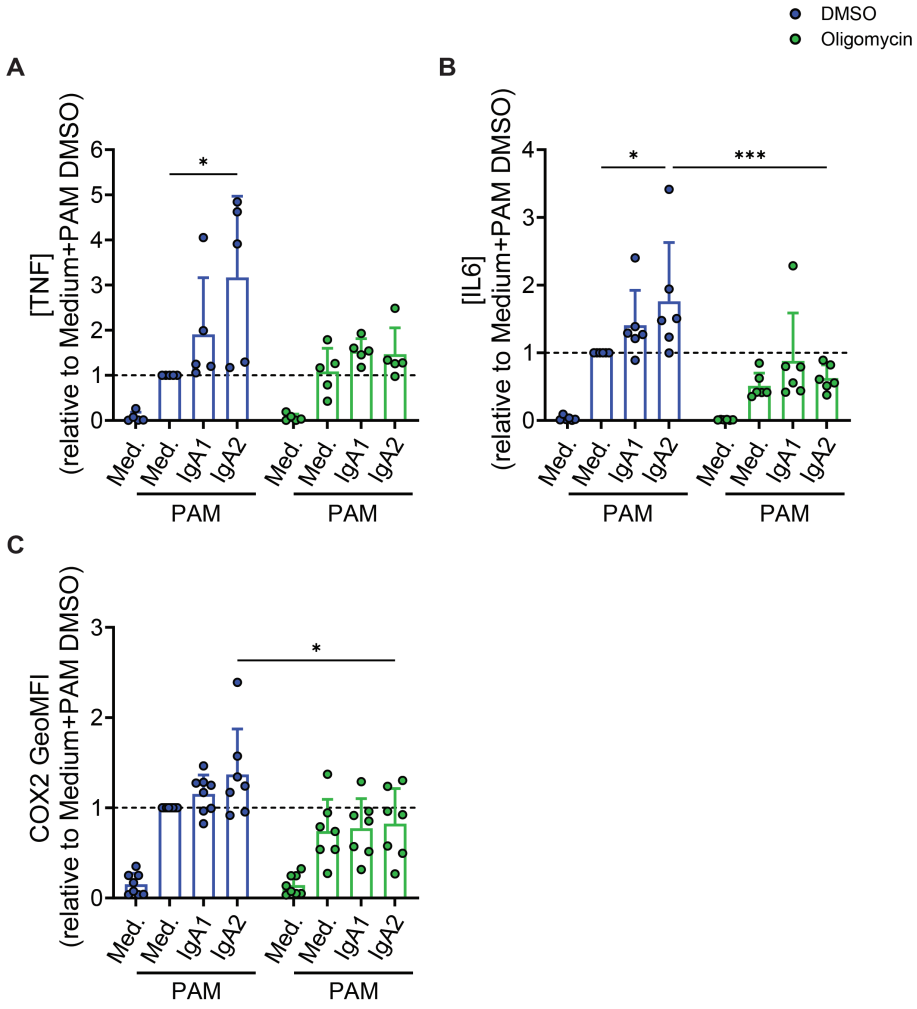

Fig3: **Inhibition of ATP Synthase with oligomycin abrogates the pro-inflammatory potentiation effects of IgA2.** Levels of (A) TNF and (B) IL-6 measured in supernatants with ELISA following stimulation of cells with indicated stimuli in the presence of DMSO (blue) or Oligomycin (green). (C) Normalized COX2 GeoMFI of cells treated with indicated stimuli in the presence of DMSO (blue) or Oligomycin (green). (A) is a representative plot of 5 donors from 3 independent experiments (mean ± SD). (B) is a representative plot of 6 donors from 3 independent experiments (mean ± SD). (C) is a representative plot of 8 donors from 4 independent experiments with outliers removed (mean ± SD). All data were analysed using a paired two-way ANOVA, with matched values both stacked and spread across a row, using a Tukey's multiple comparisons test, with a single pooled variance. * $p < 0.05$, *** $p < 0.001$.

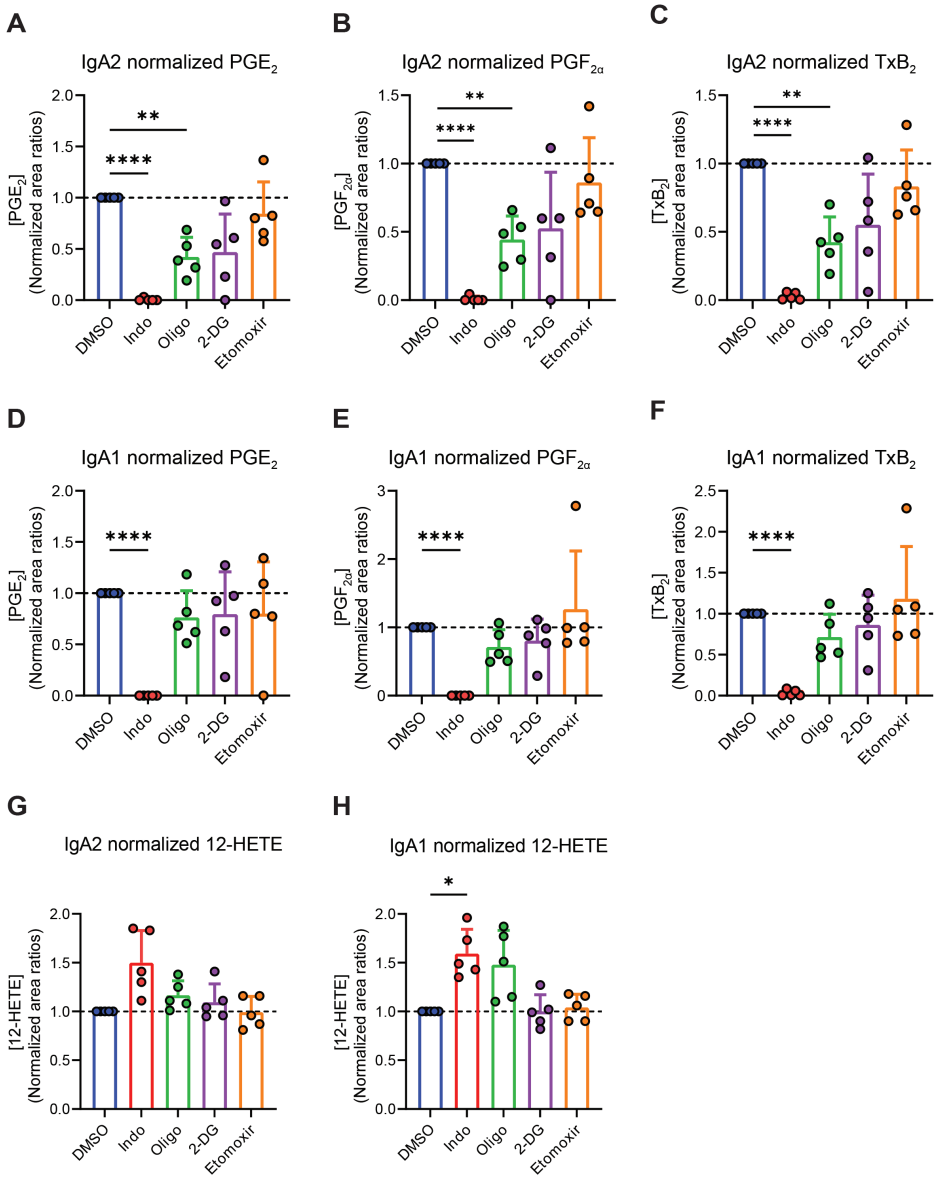

Fig4: **IgA2 requires ATP Synthase for potentiation of PAM-driven synthesis of COX2-dependent lipid mediators.** Levels of (A) PGE_2, (B) $PGF_{2\alpha}$, and (C) TxB_2 measured in supernatants of cells co-stimulated with IgA2 and PAM and indicated inhibitors. Levels of (D) PGE_2, (E) $PGF_{2\alpha}$, and (F) TxB_2 measured in supernatants of cells co-stimulated with IgA1 and PAM and indicated inhibitors. Levels of COX2-independent 12-HETE measured in supernatants of cells co-stimulated with PAM and (G) IgA2, or (H) IgA1, and indicated inhibitors. (A)-(H) are representative plots of 5 donors from 2 independent experiments (mean ± SD). All data were analysed using a paired one-way ANOVA with Dunnett's post-hoc test. The mean of each column was compared with the mean of the control column (DMSO). * $p < 0.05$, ** $p < 0.01$, **** $p < 0.0001$.

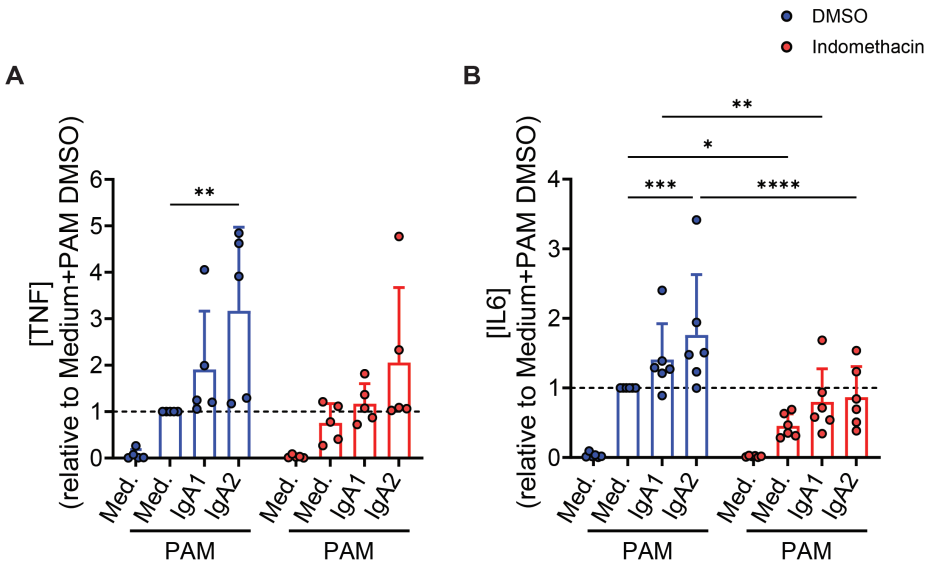

Fig5: **IgA2 requires COX2 activity for potentiation of TLR-induced cytokine production.** Levels of (A) TNF and (B) IL-6 measured in supernatants with ELISA following stimulation of cells with indicated stimuli in the presence of DMSO (blue) or Indomethacin (red). (A) is a representative plot of 5 donors from 3 independent experiments (mean ± SD). (B) is a representative plot of 6 donors from 3 independent experiments (mean ± SD). Respective DMSO controls are the same as the ones shown in Fig3. All data were analysed using a paired two-way ANOVA, with matched values both stacked and spread across a row, using a Tukey's multiple comparisons test, with a single pooled variance. * $p < 0.05$, ** $p < 0.01$, *** $p < 0.001$, **** $p < 0.0001$.

Discussion

Previous studies have shown that IgA2 drives stronger pro-inflammatory signalling in both macrophages and neutrophils, compared to IgA1 (5). Correspondingly, higher ratios of IgA2:IgA1 ACPA have been correlated with worse RA scores (5), pointing to a more detrimental role of IgA2 than IgA1 in RA pathology. In our study we have further extended these findings, by showing that, in macrophages, IgA2 ACPA has the ability to induce higher levels of TNF and IL-6, both when compared to TLR-2 ligation alone or TLR-2 and IgA1 ACPA co-stimulation. Furthermore, we also found that this increased inflammatory signalling was associated with both higher expression of COX2 and higher levels of COX2-dependent lipid mediators, specifically PGE_2. Interestingly, while no major changes were seen in OCR or Glycolysis, IgA2 did show a decrease in respiratory spare capacity. These data showing reduced spare capacity align with previous work done by van den Bossche *et al* (34) showing that M1-polarized macrophages both present some mitochondrial disfunction and display a lower metabolic elasticity, unlike M2 which can more easily adapt their metabolism if one pathway is blunted. However, despite a lack of clear reprogramming of core

metabolic pathways by these macrophages, we observed a dependence of IgA2 on ATP Synthase for TLR-induced cytokine production, COX2 expression and subsequent PGE_2 levels. We also report that indomethacin, a general COX2 inhibitor, was able to reduce the inflammatory potential of IgA2.

The distinct inflammatory effects of IgA2 and IgA1 have been postulated to be driven by differences in their glycosylation profiles. These differences may alter interaction strength with the FcαR, and thus also downstream signalling pathways, and ultimately TLR-induced cytokine production. IgA has been shown to also signal via MAPK and MyD88 (35,36), which are known mediators of TLR-driven cytokine responses and COX2 expression (37–42). This overlap of signalling pathways, together with the recent findings that IgA2 induces stronger binding and activating signalling than IgA1 (5), could explain why IgA2 induces higher expression of COX2 and drives a stronger inflammatory response than IgA1.

We have previously shown that IgA-ICs induce, and depend on, glycolytic reprogramming to render tolerogenic DCs proinflammatory (15), with no effect or dependency on mitochondrial metabolism. In contrast, our current observations in macrophages show no role for glycolysis, but instead point to a crucial role for mitochondrial ATP synthase in supporting the pro-inflammatory effects of IgA2. This is in line with other studies that have shown that in a L929 fibrosarcoma cell line, a functional electron transport chain (ETC) is required for proper NFκB activation, and TNF and IL-6 synthesis. Furthermore, tampering with either ETC complexes or ATP Synthase resulted in a reduction of these cytokines in whole blood (43,44). An additional explanation as to why ATP synthase is required for IgA2-driven inflammatory responses in macrophages, may be connected to mTOR and its role in cytokine and COX2 expression, and promotion of inflammation (42,45). Since mTOR is inhibited in conditions of low ATP:AMP ratio, it is conceivable that oligomycin, by blocking ATP synthase, decreases the ATP:AMP ratio, leading to mTOR inhibition and thus lower cytokine and COX2 expression. This, however, remains to be explored in future studies.

Additionally, work by Sanin *et al* (33) showed an effect of PGE_2 on mitochondrial membrane potential, which in turn affected gene expression in macrophages. However, in our work, we did not find alterations in membrane potential despite high levels of PGE_2 production. This can probably be explained by differences in macrophage models used, as the authors used murine M2-like macrophages from MCSF (macrophage colony-stimulating factor) cultures, while in our study we used human GM-CSF stimulated M1-like macrophages, which have been shown to respond differently to inflammatory signals (46).

Interestingly, it was shown that, in RA synoviocytes, mitochondrial dysfunction increases COX2 expression (47). In these studies, it was indicated that oligomycin increased ROS (reactive oxygen species) production, which in turn stimulated the expression of COX2, again indicating that different cell types can respond in opposite ways to the same metabolic manipulation (14).

As shown previously for IgG, IgA, and IgE (Immunoglobulin E) stimulation of monocytes (48,49), we here report that IgA2 synergizes with TLR ligands to promote COX2 and PGE_2 synthesis, and that the former is required for boosting the proinflammatory profile of macrophages induced by IgA2. However, how COX2 achieves this, in an apparently PGE_2-independent manner, remains to be determined. Possibly, there is another COX2-dependent mediator responsible for the IgA2-induced inflammation, or the effects of PGE_2 are time- and/or dose-dependent in a way that cannot be mimicked by a single supplementation in culture. This phenomenon has previously been shown in different contexts, where PGE_2 plays distinct roles depending on the concentration and the stimulation timepoint (50–53). Our data also showed $PGF_{2\alpha}$ and TxB_2 to be decreased following oligomycin treatment, as such one could speculate that one of these plays a role in supporting the proinflammatory effect of IgA2. Indeed, it was shown that both $PGF_{2\alpha}$ and Thromboxane A_2 (the active precursor of TxB_2) are present in higher levels in patients with RA compared to either healthy controls or RA patients undergoing treatment (54–56). Furthermore, previous studies suggest that prostaglandin I_2, another lipid mediator downstream of COX2, plays a role in driving inflammation in the context of RA (57,58), identifying prostaglandin I_2 as another interesting candidate to further study in the context of IgA2-driven inflammation.

In conclusion, we find a crucial role for mitochondrial ATP synthase-dependent COX2 induction in promoting a proinflammatory cytokine response following co-stimulation with PAM and IgA2, revealing a novel interplay between metabolism, lipid mediator production and cytokine expression that shapes the inflammatory profile of macrophages. Thus, our work warrants exploration of the potential of targeted manipulation of macrophage mitochondrial metabolism, as a novel strategy, to dampen IgA-driven inflammation in inflammatory disorders, such as RA.

Materials and Methods

Generation of IgA1 ACPA and IgA2 ACPA

All monoclonal antibodies had identical variable domains corresponding to the anti-citrullinated protein antibody (ACPA) clone 1C11. This clone was derived from cyclic citrullinated protein 2 (CCP2) reactive B-cells, isolated by single-cell sorting from an

ACPA-positive patient. The heavy and light chain variable domains of the B-cell receptor were sequenced as previously described (59). The ACPA 1C11 IgA variable gene sequences, linked to the lambda light chain (LC), IgA1 heavy chain (HC), or IgA2m1 HC constant domains, along with the leader peptides MELGLSWVFLVVILEGVQC (for HC) or MAWIPLFLGVLAYCTDIWA (for LC), the Kozak sequence, and BamHI and XhoI restriction sites, were codon-optimized by GeneArt (Life Technologies) and ordered from IDT. The 1C11 IgA HC and LC constructs were cloned into the pcDNA3.1(+) expression vector and co-transfected into FreestyleTM 293-F cells (Gibco) as previously reported (60). Supernatants from transfected and non-transfected cells (as negative controls) were collected and 0.45 µM filtered 5–6 days later. The supernatants were then diluted to achieve an IgA concentration of 2 µg/mL, as measured by ELISA using light chain detection antibody to check for equal coating.

Coating of plates with IgA1 ACPA or IgA2 ACPA

For regular culture and stimulation, 96-well streptavidin microplates (Microcoat, Bavaria) were coated with 50 µL of 1 µg/mL biotinylated CCP2 antigen in sterile PBS/0.1% BSA for 1h at room temperature. After 3 washes with 150 µL sterile PBS, 50 µL of IgA1, IgA2 or negative control HEK cell supernatant (Med.) were added and incubated for 1h at 37°C. The plate was washed 3 times with sterile PBS prior adding the cells.

For seahorse and SCENITH experiment, untreated 6 well culture plates (Corning) were coated with 1.5 mL of 1 µg/mL streptavidin (Invitrogen) in sterile coating buffer (0.1 M Na2CO3 0.1 M NaHCO3 in H_2O Mili-Q) and incubated overnight at 4°C. After 3 washes with 2 mL sterile PBS, 1 mL of 1 µg/mL biotinylated CCP2 antigen in sterile PBS/0.1% BSA were added per well. The wells were washed 3 times with 2 mL sterile PBS and 800 µL of HEK cell supernatant were added for 1h at 37°C. the wells were washed 3 more times with sterile PBS prior cells stimulation.

Lambda Light Chain ELISA

96-well streptavidin microplates (Microcoat, Baviera) were coated as described above. 50 µL of Sheep anti-lambda-light chain-HRP (polyclonal, abcam) in PBS/0.05% Tween/1% BSA were added for 1h at 37°C. The plate was washed 3 times with PBS/0.05% Tween and absorbance was measured at 415 nm using ABTS and H_2O_2 (Fig. S1 A-C).

Human Macrophage culture and stimulation

Peripheral blood mononuclear cells were isolated from the venous blood of healthy volunteers by density centrifugation in Ficoll as described before (61). Monocytes were isolated by positive magnetic cell sorting using CD14-microbeads (Miltenyi Biotech, 130-097-052) and cultured in complete RPMI medium (RPMI containing 10% FCS, 100 U/mL penicillin/streptomycin, and 2 mM L-glutamine) supplemented with

20 ng/mL rGM-CSF (ThermoFisher, PHC2011). On day 2/3, the medium, including supplements, was replaced.

Macrophages were stimulated on day 5 in the presence or absence (if indicated) of 2 µg/mL PAM3CSK4 (InvivoGen, tlrl-pms) in wells previously coated with HEK cell medium, IgA1 or IgA2, along with the indicated reagents: 50 µM Indomethacin (Sigma-Aldrich, I7378), 2 µM Oligomycin (Cayman, 11342), 1 µM 2-DG (Sigma-Aldrich, D8375), 3 µM Etomoxir (Sigma-Aldrich, E1905), 1 µM Entosplenetinib (SelleneckChem, S7523), 10 µM Prostaglandin E_2 (Cayman, 14010).
After 24h of stimulation, supernatant was collected and stored at -20°C, if for ELISA, or at -80°C, if for lipidomics. Cells were harvested and stained with the viability dye Zombie NIR (Biolegend, 423106) for 15 minutes at 4°C in the dark, before being fixed with 2% PFA for 10 minutes, in the dark, at room temperature.

Staining protocol and analysis

Fixed cells were washed once in 1x permeabilization buffer (ThermoFisher, 00-5523-00) before staining intracellular targets in 1x permeabilization buffer, containing Fc-block, for 2 h in the dark at room temperature. The expression of intercellular enzymes was determined by flow cytometry (Aurora; Cytek, Amsterdam, The Netherlands) using the following antibodies: COX2 (clone AS67, BD 565125), ACC1, (Abcam, ab272704), FASN (Abcam, ab128870), CPT1A (Abcam, ab235841) CS (Abcam, ab129088). Only single live cells that were negative for Zombie NIR were included in the analysis. Gating strategy and FMOs can be seen in Fig. S8. The acquired samples were unmixed using SpectroFlo version 3 and analysed with FlowJo version 10.10.0.

TNF and IL6 cytokine ELISA

Supernatants from cell cultures stored at -20°C were slowly thawed at 37°C and used to measure concentration of TNF, with BD OptEIA™ Human TNF ELISA Set (BD Biosciences, 555212), and IL-6, with BD OptEIA™ Human IL-6 ELISA Set (BD Biosciences, 555220) according to manufacturer instructions.

Measurement of lipid mediators

Lipid mediators (LMs) and polyunsaturated fatty acids (PUFA) were measured using reverse-phase liquid chromatography coupled to tandem mass spectrometry (RPLC-MS/MS) as previously described (62), with some modifications. Briefly, 2 µL internal standard (IS) mix of deuterated lipid standards consisting of PGE_2-d_4, 15-HETE-d_8, Leukotriene B_4-d_4, DHA-d_5, 8-iso-$PGF_{2\alpha}$-d_4, and 14(15)-EET-d_{11} (50 ng/mL in methanol (MeOH)) was added to 400 µL culture supernatants. Lipids were extracted and purified by solid-phase extraction (SPE) after protein precipitation with 1.2 mL MeOH. The dried extracts were reconstituted in 100 µL 40% MeOH and transferred into a micro-vial glass insert. Furthermore, a 40-µL sample was injected and analysed using a Shimadzu Nexera LC40 system with an autosampler coupled to a QTrap 6500 mass

spectrometer (Sciex). Kinetex C18 50 × 2.1 mm, 1.7 µm column, and C8 precolumn (Phenomenex) were used for LC separation. LC–MS/MS chromatograms were integrated manually using Sciex OS (Sciex). The results were reported as relative peak area of lipids to the internal standards. PGE_2-d_4 IS was used for reporting the area ratios of PGE_2, TxB_2, and $PGF_{2\alpha}$.

Extracellular Flux Assay (Seahorse)

5×10^5 macrophages were plated in an XFe96 well Seahorse plate (Agilent) after being stimulated overnight. Medium was replaced, after washing 2x with PBS, with 180 µL XF assay made from base RPMI without HEPES and $NaHCO_3$ (Sigma, R6504) supplemented with 5% FCS and 2 mM L-Glutamine, and incubated in a non-CO_2 37 °C incubator for 1 h. As cells were incubating, injected compounds were diluted in XF media (without FCS) and added to the hydrated cartridge, after which the cartridge was immediately loaded into the Seahorse for calibration. 10 mM Glucose (Sigma, G8644), 1,5 µM Oligomycin (Cayman, 11342), 3 µM FCCP (Sigma, C2920), 1 µM Rotenone (Sigma, 557368) and 1 µM Antimycin A (Sigma, A8674).

Homopropargylglycine uptake (SCENITH)

$5x10^5$ macrophages were plated in a 96-well untreated V-bottom plate, washed with PBS, and plated in 90 µL of methionine-free medium (Sigma, R7513) supplemented with 65 mg/L L-cystine dihydrochloride (Sigma, C6727), 2 mM L-Glutamine (Sigma, G3126), and 10% dialyzed FCS (ThermoFisher, A3382001). Cells were starved of methionine for 45 min at 37°C, before addition of 10 µl of indicated inhibitor(s) (medium, 2 µM Oligomycin, 100 mM 2DG, or 2 µM Oligomycin and 100 mM 2DG) and subsequently incubated another 15 min at 37°C. Homopropargylglycine (Click Chemistry Tools, 1067) was added at a final concentration of 100 µM and incubated for 30 min at 37°C before being washed 2x with cold PBS, live/dead stain with Zombie NIR at 4°C for 15 minutes, washed 2x with cold PBS, and fixed with 2% PFA for 10 min.

Click Chemistry Reaction

Cells fixed after Homopropargylglycine uptake were permeabilized with PBS containing 1% BSA/0.1% Saponin for 15 min and washed 2x in Click buffer (100 mM Tris-HCl, pH 7.4) before the addition of Click reaction mix. The reaction mix was made by sequential addition of 10 mM Sodium Ascorbate (Sigma, A7631), 2 mM THPTA (Click Chemistry Tools, 1010), 0.5 µM AFdye488 azide plus (Click Chemistry Tools, 1475) and 1x click buffer to $CuSO_4$ (0.5 mM final conc., [Sigma, 209198]). Samples were incubated for 30 min in the dark at room temperature. Cells were washed with FACS buffer and measured on the Aurora. The acquired samples were unmixed using SpectroFlo version 3 and analysed with FlowJo version 10.10.0. Calculations of metabolic capacities and dependences were done as previously described (63).

Statistical Analysis

The statistical tests used are indicated in the figure legends. Generally, data were compared using one-way ANOVA for more than two groups or two-way ANOVA for comparing multiple parameters across two or more groups, with Tukey's *post-hoc* test for multiple comparison. *p*-values <0.05 were considered significant ($*p<0.05$, $**p<0.01$, $***p<0.001$, $****p<0.0001$). All statistical analyses were performed using GraphPad Prism v.10.2.3.

Data Availability Statement

The data that support the findings of this study are available from the corresponding author upon reasonable request.

Conflict of Interest

The authors declare no conflict of interest.

Ethics Statement

The studies involving humans were approved by Sanquin National Blood donation Bank. The studies were conducted in accordance with the local legislation and institutional requirements. The human samples used in this study were acquired from voluntary blood donations to Sanquin Blood bank. Written informed consent for participation was not required from the participants or the participants' legal guardians/ next of kin in accordance with the national legislation and institutional requirements.

Author contributions

LA: Formal analysis, Investigation, Methodology, Visualization, Writing – original draft. AB: Formal Analysis, Investigation, Methodology, Writing – review & editing. MGh: Data curation, Formal Analysis, Investigation, Methodology, Writing – review & editing. AH: Investigation, Methodology, Writing – review & editing. RT: Conceptualization, Resources, Supervision, Writing – review & editing. MGi: Conceptualization, Resources, Supervision, Writing – review & editing. BE: Conceptualization, Funding acquisition, Project administration, Supervision, Writing – original draft.

Acknowledgements

Many thanks to Dr. Jeroen den Dunnen, Chiara Geyer, and Lynn Mes for their support and collaboration. We would also like to thank our colleagues from the Leiden

University Centre for Infectious Diseases, and Dr. Luís Almeida from Mainz University for their continual scientific discussions. We would also like to acknowledge the LUMC Flow Core Facility operators for the continual maintenance and troubleshooting of the Cytek Auroras.

This work was supported by funding from the European Union's Horizon 2020 research and innovation programme under the Marie Skłodowska-Curie Grant agreement No. 812890.

Supplementary Materials

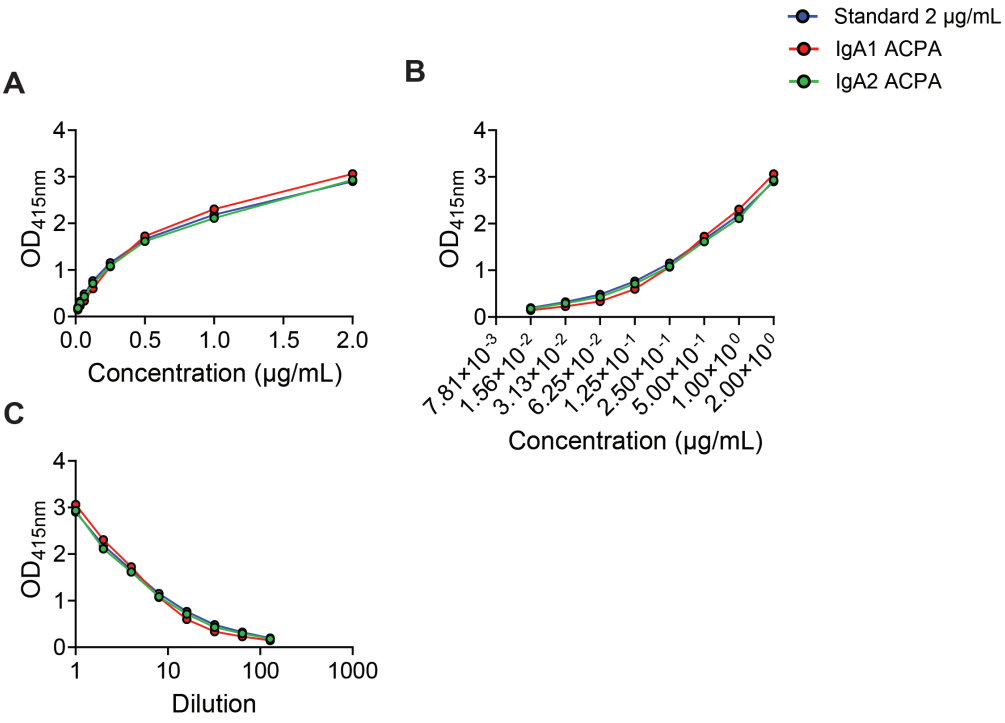

Fig. S1: **Coating of the monoclonal IgA1 ACPA and IgA2 ACPA.** Antibody binding to the CCP2 antigen was measured by ELISA using anti-lambda light chain detection antibody as described in materials and methods. Optical Density at 415nm (OD_{415nm}) and corresponding linear (A) and log_2 (B) concentration of antibody used. (C) Optical Density at 415nm and corresponding log_{10} dilution. (A)-(C) are representative plots of 2 replicates from 1 experiment (mean ± SD).

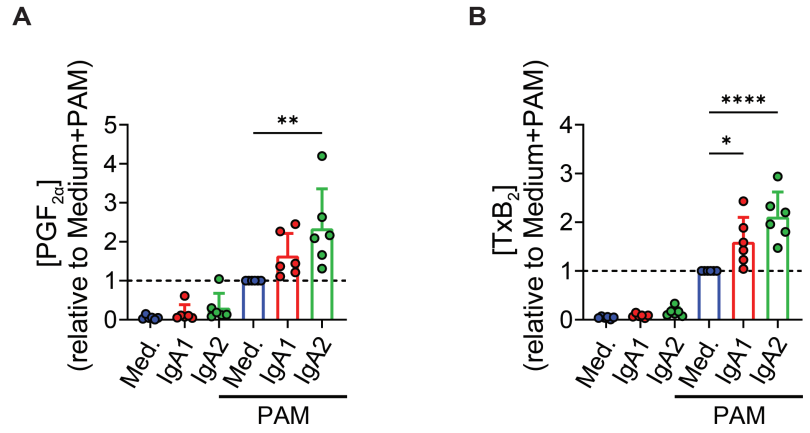

Fig. S2: **IgA synergizes with PAM to potentiate synthesis of COX2-dependent lipid mediators.** Levels of (A) $PGF_{2\alpha}$, and (B) TxB_2 measured in supernatants following stimulation of cells with indicated compounds. (A)-(B) are representative plots of 6 donors from 2 independent experiments (mean ± SD). All data were compared using an ordinary one-way ANOVA. * $p < 0.05$, ** $p < 0.01$, **** $p < 0.0001$.

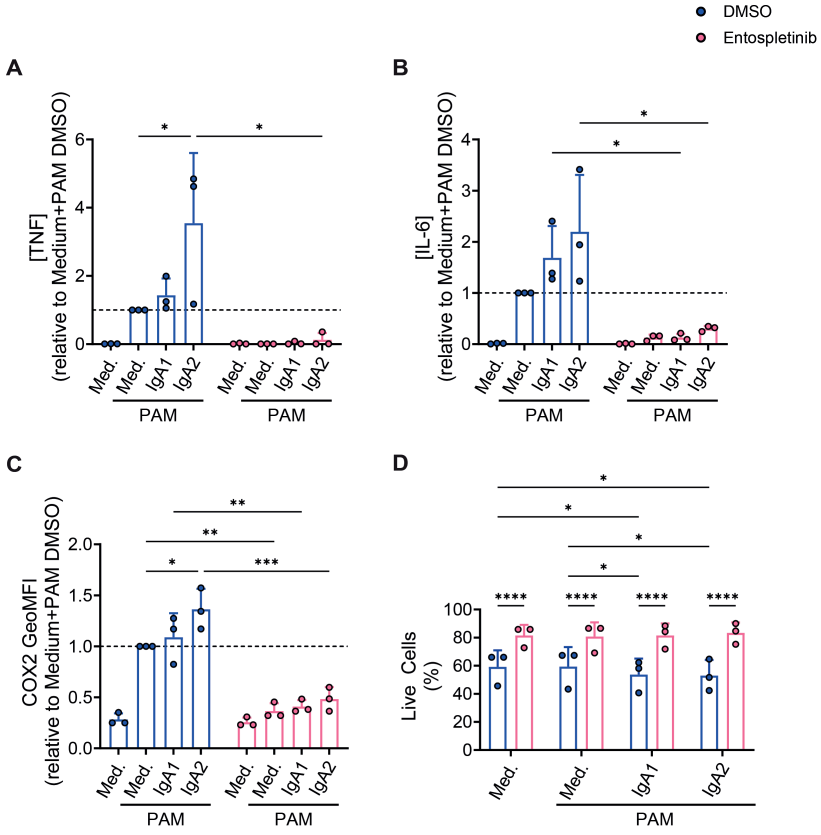

(legend on next page)

Fig. S3: **IgA1 and IgA2 signal through Syk.** Levels of (A) TNF and (B) IL-6 measured in supernatants with ELISA following stimulation of cells with indicated stimuli in the presence of DMSO (blue) or the Syk inhibitor Entospletinib (lilac). (C) Normalized COX2 GeoMFI of cells treated with indicated stimuli in the presence of DMSO (blue) or Entospletinib (lilac). (D) Viability of cells treated with indicated stimuli in the presence of DMSO (blue) or Entospletinib (lilac). (A)-(D) are representative plots of 3 donors from 2 independent experiments (mean ± SD). All data were analysed using a paired two-way ANOVA, with matched values both stacked and spread across a row, using a Tukey's multiple comparisons test, with a single pooled variance. * p < 0.05, ** p < 0.01, *** p < 0.001, **** p < 0.0001.

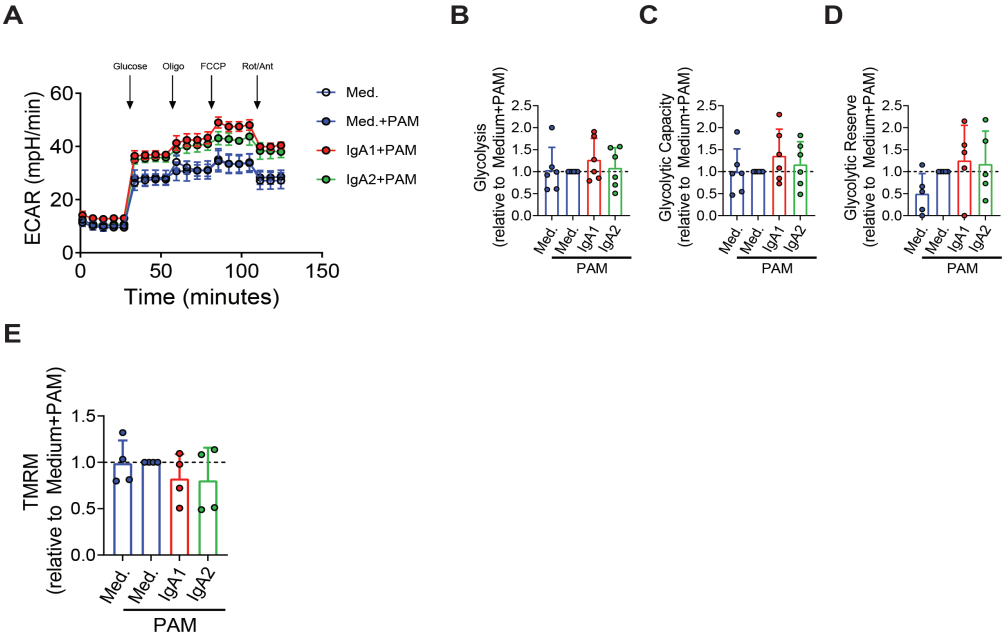

Fig. S4: **IgA2-PAM co-stimulation does not affect glycolysis or mitochondrial membrane potential.** (A) Representative plot of extracellular acidification rate (ECAR) of cells stimulated for 24h with indicated stimuli, measured using an extracellular flux analyser (Seahorse). (B) Basal glycolysis, (C) Glycolytic capacity, and (D) Glycolytic reserve. (E) Mitochondrial membrane potential measured with TMRM (Tetramethylrhodamine). (A)-(D) are representative plots of 6 donors from 3 independent experiments with outliers removed (mean ± SD). (E) is a representative plot of 4 donors from 2 independent experiments (mean ± SD). All data were analysed using a paired one-way ANOVA.

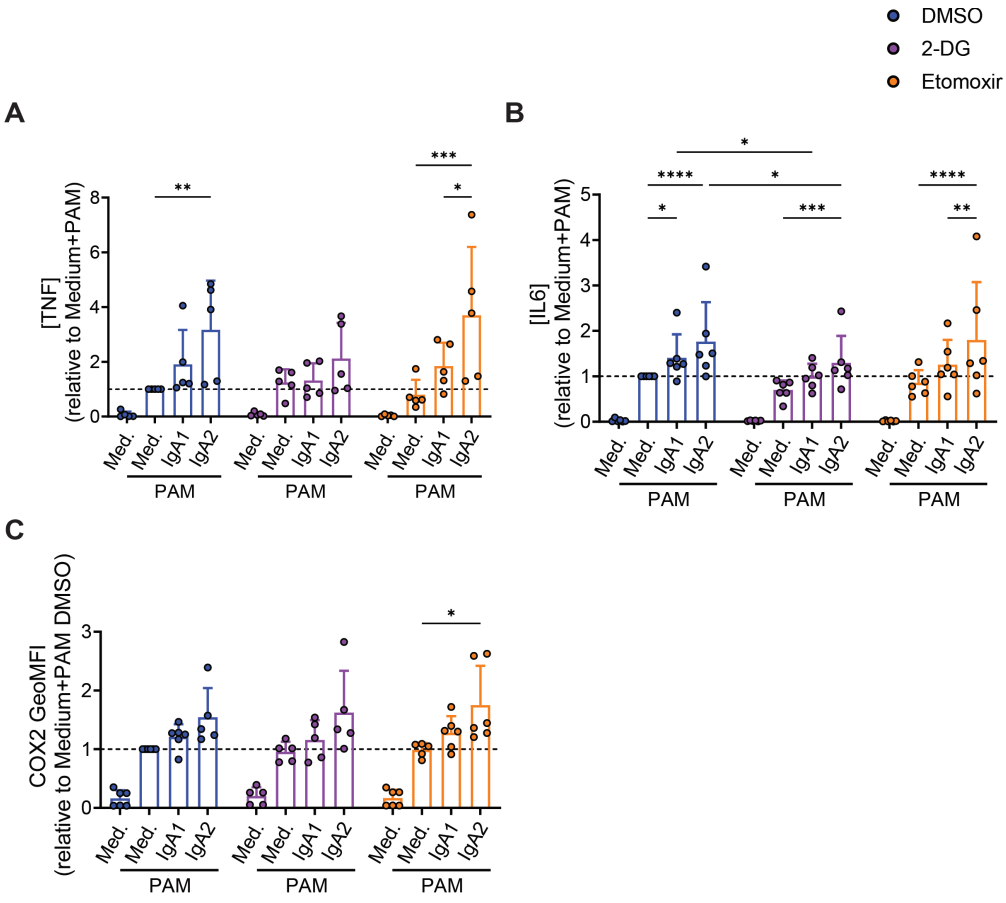

Fig. S5: **Inhibition of glycolysis with 2-DG or inhibition of fatty acid oxidation with Etomoxir does not affect IgA1- and IgA2-dependent inflammation.** Levels of (A) TNF and (B) IL-6 measured in supernatants with ELISA following stimulation of cells with indicated stimuli in the presence of DMSO (blue), 2-DG (purple) or Etomoxir (orange). (C) Normalized COX2 GeoMFI of cells treated with indicated stimuli in the presence of DMSO (blue), 2-DG (purple) or Etomoxir (orange). (A) is a representative plot of 5 donors from 3 independent experiments (mean ± SD). (B)-(C) are representative plots of 6 donors from 3 independent experiments with outliers removed (mean ± SD). Respective DMSO controls are the same as the ones shown in Fig3. All data were analysed using a paired two-way ANOVA, with matched values both stacked and spread across a row, using a Tukey's multiple comparisons test, with a single pooled variance. * $p < 0.05$, ** $p < 0.01$, *** $p < 0.001$, **** $p < 0.0001$.

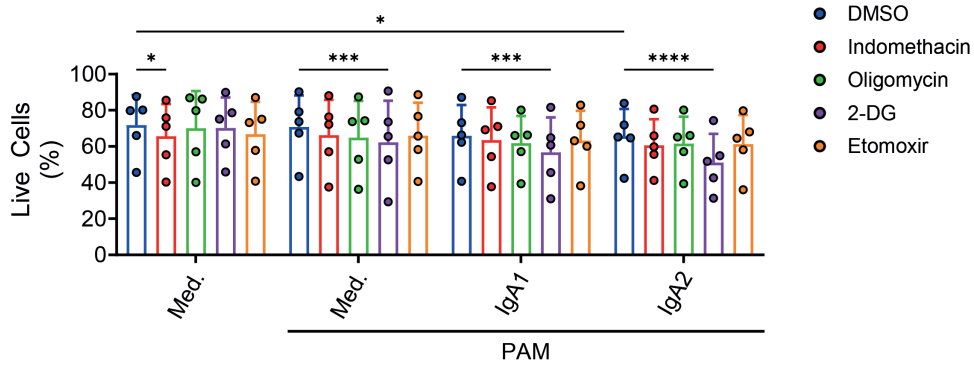

Fig. S6: **Viability of inhibitor-treated cells.** Viability of cells treated with indicated stimuli in the presence of DMSO (blue), Indomethacin (red), Oligomycin (green), 2-DG (purple) or Etomoxir (orange), measured with flow cytometry following Live/Dead staining with Zombie NIR as described in materials and methods. Representative plots of 5 donors from 3 independent experiments (mean ± SD). Data were analysed using a paired two-way ANOVA, with matched values both stacked and spread across a row, using a Tukey's multiple comparisons test, with a single pooled variance. * $p < 0.05$, *** $p < 0.001$, **** $p < 0.0001$.

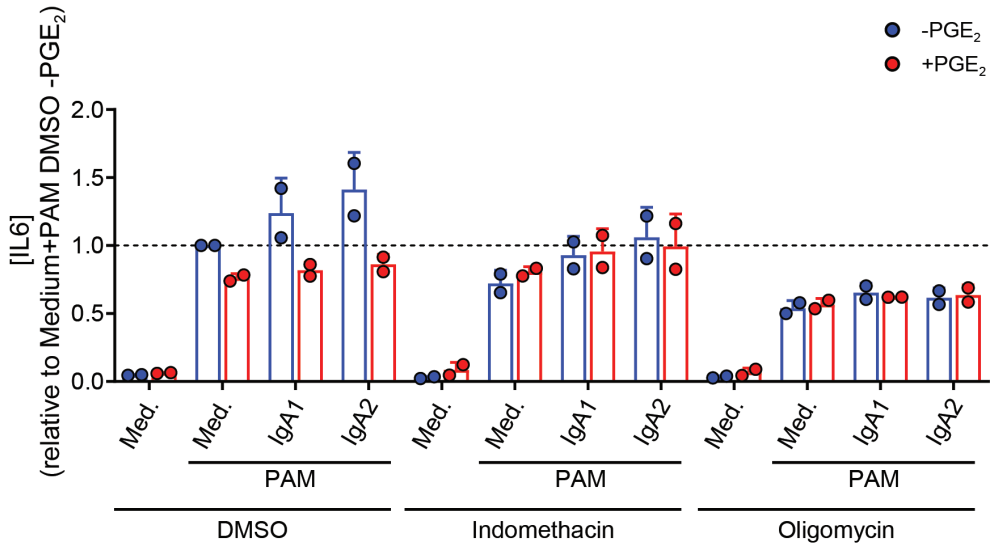

Fig. S7: **Pro-inflammatory potentiation driven by IgA2 is independent of PGE2.** Levels of IL-6 measured in supernatants following stimulation of cells with indicated stimuli in the absence (blue) or presence (red) of exogenous PGE2. Representative plot of 2 donors from 1 experiment (mean ± SD).

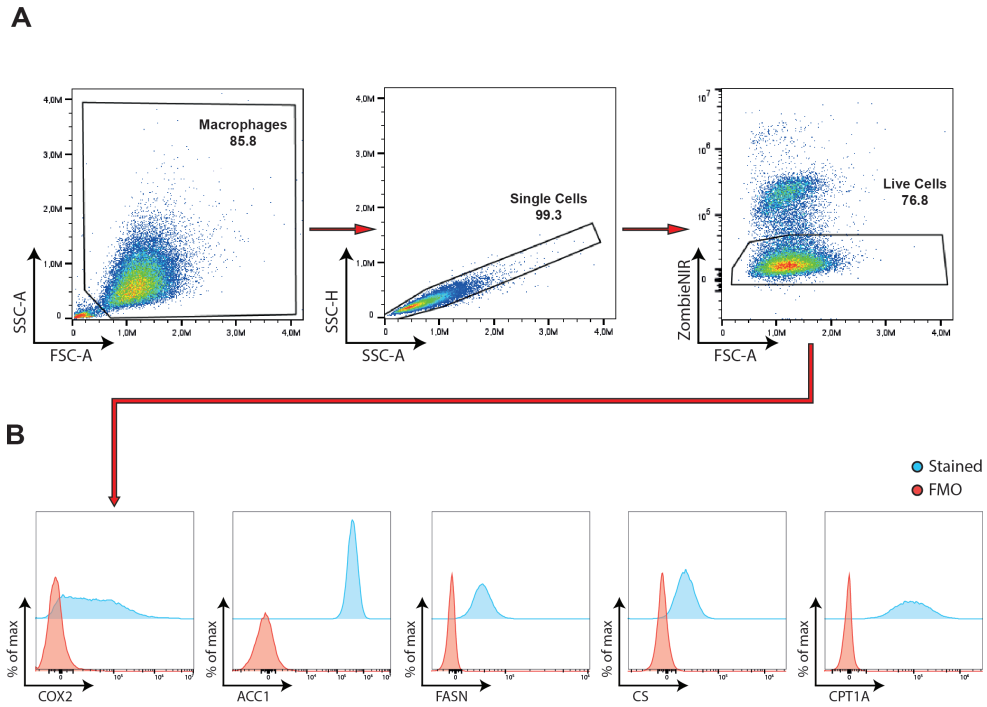

Fig. S8. **Gating strategy and FMOs.** Cells were gated according to FSC-A and SSC-A parameters (A), followed by exclusion of doublets, and selection of live cells, according to Zombie NIR staining. (B) Expression of COX2, ACC1, FASN, CS, and CPT1A, measured via flow cytometry, in live PAM-treated GM-CSF macrophages, compared to respective FMO (Fluorescence Minus One) controls.

References

1. Dingess KA, Hoek M, van Rijswijk DMH, Tamara S, den Boer MA, Veth T, et al. Identification of common and distinct origins of human serum and breastmilk IgA1 by mass spectrometry-based clonal profiling. Cell Mol Immunol. 2023 Jan;20(1):26–37.

2. Bunker JJ, Bendelac A. IgA Responses to Microbiota. Immunity. 2018 Aug 21;49(2):211–24.

3. Kerr MA. The structure and function of human IgA. Biochem J. 1990 Oct 15;271(2):285–96.

4. Hansen IS, Hoepel W, Zaat SAJ, Baeten DLP, den Dunnen J. Serum IgA Immune Complexes Promote Proinflammatory Cytokine Production by Human Macrophages, Monocytes, and Kupffer Cells through FcαRI–TLR Cross-Talk. The Journal of Immunology. 2017 Dec 15;199(12):4124–31.

5. Steffen U, Koeleman CA, Sokolova MV, Bang H, Kleyer A, Rech J, et al. IgA subclasses have different effector functions associated with distinct glycosylation profiles. Nat Commun. 2020 Jan 8;11(1):120.

6. Mes L, Steffen U, Chen HJ, Veth J, Hoepel W, Griffith GR, et al. IgA2 immune complexes selectively promote inflammation by human CD103+ dendritic cells. Front Immunol [Internet]. 2023 Mar 16 [cited 2024 Aug 21];14. Available from: https://www.frontiersin.org/journals/immunology/articles/10.3389/fimmu.2023.1116435/full

7. Gayet R, Michaud E, Nicoli F, Chanut B, Paul M, Rochereau N, et al. Impact of IgA isoforms on their ability to activate dendritic cells and to prime T cells. European Journal of Immunology. 2020;50(9):1295–306.

8. Bacon A, Cartagena García C, van Schie KA, Toes REM, Busnel JM. A whole blood-based functional assay to characterize immunoglobulin A effector functions. Autoimmunity. 2024 Dec 31;57(1):2341629.

9. Dechant M, Beyer T, Schneider-Merck T, Weisner W, Peipp M, van de Winkel JGJ, et al. Effector mechanisms of recombinant IgA antibodies against epidermal growth factor receptor. J Immunol. 2007 Sep 1;179(5):2936–43.

10. Ohyama Y, Renfrow MB, Novak J, Takahashi K. Aberrantly Glycosylated IgA1 in IgA Nephropathy: What We Know and What We Don't Know. J Clin Med. 2021 Aug 5;10(16):3467.

11. de Sousa-Pereira P, Woof JM. IgA: Structure, Function, and Developability. Antibodies. 2019 Dec;8(4):57.

12. van Egmond M, Damen CA, van Spriel AB, Vidarsson G, van Garderen E, van de Winkel JG. IgA and the IgA Fc receptor. Trends Immunol. 2001 Apr;22(4):205–11.

13. O'Neill LAJ, Kishton RJ, Rathmell J. A guide to immunometabolism for immunologists. Nat Rev Immunol. 2016 Sep;16(9):553–65.

14. Almeida L, Everts B. Fa(c)t checking: How fatty acids shape metabolism and function of macrophages and dendritic cells. Eur J Immunol. 2021 Jul;51(7):1628–40.

15. Hansen IS, Krabbendam L, Bernink JH, Loayza-Puch F, Hoepel W, van Burgsteden JA, et al. FcαRI co-stimulation converts human intestinal CD103+ dendritic cells into pro-inflammatory cells through glycolytic reprogramming. Nat Commun. 2018 Feb 28;9(1):863.

16. Jing C, Castro-Dopico T, Richoz N, Tuong ZK, Ferdinand JR, Lok LSC, et al. Macrophage metabolic reprogramming presents a therapeutic target in lupus nephritis. Proc Natl Acad Sci U S A. 2020 Jun 30;117(26):15160–71.

17. Akter S, Sharma RK, Sharma S, Rastogi S, Fiebich BL, Akundi RS. Exogenous ATP modulates PGE2 release in macrophages through sustained phosphorylation of CDK9 and p38 MAPK. Journal of Leukocyte Biology. 2021 Oct 1;110(4):663–77.

18. Sheppe AEF, Kummari E, Walker A, Richards A, Hui WW, Lee JH, et al. PGE2 Augments Inflammasome Activation and M1 Polarization in Macrophages Infected With Salmonella Typhimurium and

Yersinia enterocolitica. Front Microbiol [Internet]. 2018 Oct 31 [cited 2024 Aug 11];9. Available from: https://www.frontiersin.org/journals/microbiology/articles/10.3389/fmicb.2018.02447/full

19. Wang W, Liang M, Wang L, Bei W, Rong X, Xu J, et al. Role of prostaglandin E2 in macrophage polarization: Insights into atherosclerosis. Biochemical Pharmacology. 2023 Jan 1;207:115357.

20. Minghetti L. Cyclooxygenase-2 (COX-2) in inflammatory and degenerative brain diseases. J Neuropathol Exp Neurol. 2004 Sep;63(9):901–10.

21. Caspi D, Anouk M, Golan I, Paran D, Kaufman I, Wigler I, et al. Synovial fluid levels of anti-cyclic citrullinated peptide antibodies and IgA rheumatoid factor in rheumatoid arthritis, psoriatic arthritis, and osteoarthritis. Arthritis Rheum. 2006 Feb 15;55(1):53–6.

22. Sokolova MV, Hagen M, Bang H, Schett G, Rech J, Steffen U, et al. IgA anti-citrullinated protein antibodies are associated with flares during DMARD tapering in rheumatoid arthritis. Rheumatology (Oxford). 2022 May 5;61(5):2124–31.

23. Roh JS, Sohn DH. Damage-Associated Molecular Patterns in Inflammatory Diseases. Immune Netw. 2018 Aug;18(4):e27.

24. Fuentelsaz-Romero S, Cuervo A, Estrada-Capetillo L, Celis R, García-Campos R, Ramírez J, et al. GM-CSF Expression and Macrophage Polarization in Joints of Undifferentiated Arthritis Patients Evolving to Rheumatoid Arthritis or Psoriatic Arthritis. Front Immunol. 2021 Feb 17;11:613975.

25. Soler Palacios B, Estrada-Capetillo L, Izquierdo E, Criado G, Nieto C, Municio C, et al. Macrophages from the synovium of active rheumatoid arthritis exhibit an activin A-dependent pro-inflammatory profile. J Pathol. 2015 Feb;235(3):515–26.

26. Sierra-Filardi E, Puig-Kröger A, Blanco FJ, Nieto C, Bragado R, Palomero MI, et al. Activin A skews macrophage polarization by promoting a proinflammatory phenotype and inhibiting the acquisition of anti-inflammatory macrophage markers. Blood. 2011 May 12;117(19):5092–101.

27. Puig-Kröger A, Sierra-Filardi E, Domínguez-Soto A, Samaniego R, Corcuera MT, Gómez-Aguado F, et al. Folate receptor beta is expressed by tumor-associated macrophages and constitutes a marker for M2 anti-inflammatory/regulatory macrophages. Cancer Res. 2009 Dec 15;69(24):9395–403.

28. Al-Mossawi MH, Chen L, Fang H, Ridley A, de Wit J, Yager N, et al. Unique transcriptome signatures and GM-CSF expression in lymphocytes from patients with spondyloarthritis. Nat Commun. 2017 Nov 15;8(1):1510.

29. Cook AD, Braine EL, Campbell IK, Rich MJ, Hamilton JA. Blockade of collagen-induced arthritis post-onset by antibody to granulocyte-macrophage colony-stimulating factor (GM-CSF): requirement for GM-CSF in the effector phase of disease. Arthritis Res. 2001;3(5):293–8.

30. Santegoets KCM, Wenink MH, Berg WB van den, Radstake TRDJ. Fc Gamma Receptor IIb on GM-CSF Macrophages Controls Immune Complex Mediated Inhibition of Inflammatory Signals. PLOS ONE. 2014 Oct 23;9(10):e110966.

31. Wessendarp M, Watanabe-Chailland M, Liu S, Stankiewicz T, Ma Y, Kasam RK, et al. Role of GM-CSF in regulating metabolism and mitochondrial functions critical to macrophage proliferation. Mitochondrion. 2022 Jan;62:85–101.

32. Na YR, Gu GJ, Jung D, Kim YW, Na J, Woo JS, et al. GM-CSF Induces Inflammatory Macrophages by Regulating Glycolysis and Lipid Metabolism. The Journal of Immunology. 2016 Nov 15;197(10):4101–9.

33. Sanin DE, Matsushita M, Klein Geltink RI, Grzes KM, van Teijlingen Bakker N, Corrado M, et al. Mitochondrial Membrane Potential Regulates Nuclear Gene Expression in Macrophages Exposed to Prostaglandin E2. Immunity. 2018 Dec 18;49(6):1021-1033.e6.

34. Van den Bossche J, Baardman J, Otto NA, van der Velden S, Neele AE, van den Berg SM, et al. Mitochondrial Dysfunction Prevents Repolarization of Inflammatory Macrophages. Cell Reports. 2016 Oct 11;17(3):684–96.

35. Zhang J, Mi Y, Zhou R, Liu Z, Huang B, Guo R, et al. The TLR4-MyD88-NF-κB pathway is involved in sIgA-mediated IgA nephropathy. J Nephrol. 2020 Dec 1;33(6):1251–61.

36. Park RK, Izadi KD, Deo YM, Durden DL. Role of Src in the Modulation of Multiple Adaptor

Proteins in FcαRI Oxidant Signaling. Blood. 1999 Sep 15;94(6):2112–20.

37. Park YK, Hong H, Jang BC. Transcriptional and translational regulation of COX-2 expression by cadmium in C6 glioma cells. International Journal of Molecular Medicine. 2012 Oct 1;30(4):960–6.

38. Echizen K, Hirose O, Maeda Y, Oshima M. Inflammation in gastric cancer: Interplay of the COX-2/prostaglandin E2 and Toll-like receptor/MyD88 pathways. Cancer Sci. 2016 Apr;107(4):391–7.

39. Lee IT, Lee CW, Tung WH, Wang SW, Lin CC, Shu JC, et al. Cooperation of TLR2 with MyD88, PI3K, and Rac1 in Lipoteichoic Acid–Induced cPLA2/COX-2–Dependent Airway Inflammatory Responses. The American Journal of Pathology. 2010 Apr 1;176(4):1671–84.

40. Fukata M, Chen A, Klepper A, Krishnareddy S, Vamadevan AS, Thomas LS, et al. Cox-2 is regulated by toll-like receptor-4 (TLR4) signaling and is important for proliferation and apoptosis in response to intestinal mucosal injury. Gastroenterology. 2006 Sep;131(3):862–77.

41. Zhang X, Zhang J, Yang X, Han X. Several transcription factors regulate COX-2 gene expression in pancreatic beta-cells. Mol Biol Rep. 2007 Sep;34(3):199–206.

42. Lin X, Sun Q, Zhou L, He M, Dong X, Lai M, et al. Colonic epithelial mTORC1 promotes ulcerative colitis through COX-2-mediated Th17 responses. Mucosal Immunol. 2018 Nov;11(6):1663–73.

43. Schulze-Osthoff K, Beyaert R, Vandevoorde V, Haegeman G, Fiers W. Depletion of the mitochondrial electron transport abrogates the cytotoxic and gene-inductive effects of TNF. EMBO J. 1993 Aug;12(8):3095–104.

44. Karan KR, Trumpff C, McGill MA, Thomas JE, Sturm G, Lauriola V, et al. Mitochondrial respiratory capacity modulates LPS-induced inflammatory signatures in human blood. Brain, Behavior, & Immunity - Health. 2020 May 1;5:100080.

45. Tyagi A, Kamal MA, Poddar NK. Integrated Pathways of COX-2 and mTOR: Roles in Cell Sensing and Alzheimer's Disease. Front Neurosci. 2020 Jul 9;14:693.

46. Ushach I, Zlotnik A. Biological role of granulocyte macrophage colony-stimulating factor (GM-CSF) and macrophage colony-stimulating factor (M-CSF) on cells of the myeloid lineage. J Leukoc Biol. 2016 Sep;100(3):481–9.

47. Valcárcel-Ares MN, Riveiro-Naveira RR, Vaamonde-García C, Loureiro J, Hermida-Carballo L, Blanco FJ, et al. Mitochondrial dysfunction promotes and aggravates the inflammatory response in normal human synoviocytes. Rheumatology (Oxford). 2014 Jul;53(7):1332–43.

48. Ferreri NR, Howland WC, Spiegelberg HL. Release of leukotrienes C4 and B4 and prostaglandin E2 from human monocytes stimulated with aggregated IgG, IgA, and IgE. The Journal of Immunology. 1986 Jun 1;136(11):4188–93.

49. Nitta T, Suzuki T. Fc gamma 2b receptor-mediated prostaglandin synthesis by a murine macrophage cell line (P388D1). The Journal of Immunology. 1982 Jun 1;128(6):2527–32.

50. Chapman S, Grauer E, Gez R, Egoz I, Lazar S. Time dependent dual effect of anti-inflammatory treatments on sarin-induced brain inflammation: Suggested role of prostaglandins. Neurotoxicology. 2019 Sep;74:19–27.

51. Osma-Garcia IC, Punzón C, Fresno M, Díaz-Muñoz MD. Dose-dependent effects of prostaglandin E2 in macrophage adhesion and migration. Eur J Immunol. 2016 Mar;46(3):677–88.

52. Yu J, Wu Y, Wang L, Zhang W, Xu M, Song J, et al. mPGES-1-derived prostaglandin E2 stimulates Stat3 to promote podocyte apoptosis. Apoptosis. 2017 Nov 1;22(11):1431–40.

53. Shi J, Johansson J, Woodling NS, Wang Q, Montine TJ, Andreasson K. The Prostaglandin E2 E-Prostanoid 4 Receptor Exerts Anti-Inflammatory Effects in Brain Innate Immunity. The Journal of Immunology. 2010 Jun 15;184(12):7207–18.

54. Trang LE, Granström E, Lövgren O. Levels of prostaglandins F2 alpha and E2 and thromboxane B2 in joint fluid in rheumatoid arthritis. Scand J Rheumatol. 1977;6(3):151–4.

55. Basu S, Whiteman M, Mattey DL, Halliwell B. Raised levels of F(2)-isoprostanes and prostaglandin F(2alpha) in different rheumatic diseases. Ann Rheum Dis. 2001 Jun;60(6):627–31.

56. Wang MJ, Huang Y, Huang RY, Chen XM, Zhou YY, Yu WL, et al. Determination of role of thromboxane A2 in rheumatoid arthritis. Discov Med. 2015 Jan;19(102):23–32.

57. Honda T, Segi-Nishida E, Miyachi Y, Narumiya S. Prostacyclin-IP signaling and prostaglandin E2-EP2/EP4 signaling both mediate joint inflammation in mouse collagen-induced arthritis. Journal of Experimental Medicine. 2006 Jan 30;203(2):325–35.

58. Pulichino AM, Rowland S, Wu T, Clark P, Xu D, Mathieu MC, et al. Prostacyclin Antagonism Reduces Pain and Inflammation in Rodent Models of Hyperalgesia and Chronic Arthritis. The Journal of Pharmacology and Experimental Therapeutics. 2006 Dec 1;319(3):1043–50.

59. Kissel T, Reijm S, Slot LM, Cavallari M, Wortel CM, Vergroesen RD, et al. Antibodies and B cells recognising citrullinated proteins display a broad cross-reactivity towards other post-translational modifications. Ann Rheum Dis. 2020 Apr;79(4):472–80.

60. Vink T, Oudshoorn-Dickmann M, Roza M, Reitsma JJ, de Jong RN. A simple, robust and highly efficient transient expression system for producing antibodies. Methods. 2014 Jan 1;65(1):5–10.

61. Hussaarts L, Smits HH, Schramm G, van der Ham AJ, van der Zon GC, Haas H, et al. Rapamycin and omega-1: mTOR-dependent and -independent Th2 skewing by human dendritic cells. Immunol Cell Biol. 2013 Aug;91(7):486–9.

62. Giera M, Ioan-Facsinay A, Toes R, Gao F, Dalli J, Deelder AM, et al. Lipid and lipid mediator profiling of human synovial fluid in rheumatoid arthritis patients by means of LC-MS/MS. Biochim Biophys Acta. 2012 Nov;1821(11):1415–24.

63. Argüello RJ, Combes AJ, Char R, Gigan JP, Baaziz AI, Bousiquot E, et al. SCENITH: A flow cytometry based method to functionally profile energy metabolism with single cell resolution. Cell Metab. 2020 Dec 1;32(6):1063-1075.e7.